

# Negative Differential Resistance Behavior in Conjugated Molecular Wires Incorporating Spacers: A Quantum-Chemical Description

Y. Karzazi,<sup>†</sup> J. Cornil,<sup>†,‡</sup> and J. L. Brédas<sup>\*,†,‡</sup>

Contribution from the Laboratory for Chemistry of Novel Materials, Center for Research on Molecular Electronics and Photonics, University of Mons-Hainaut, Place du Parc 20, B-7000 Mons, Belgium, and Department of Chemistry, The University of Arizona, Tucson, Arizona 85721-0041

Received January 17, 2001

**Abstract:** Recent experimental studies have demonstrated that single molecules or a small number of self-assembled molecules can perform the basic functions of traditional electronic components, such as wires and diodes. In particular, molecular wires inserted into nanopores can be used as active elements for the fabrication of resonant tunneling diodes (RTDs), whose *I/V* characteristics reveal a Negative Differential Resistance (NDR) behavior (i.e., a negative slope in the *I/V* curve). Here, quantum-chemical calculations are used to describe on a qualitative basis the mechanism leading to NDR in polyphenylene-based molecular wires incorporating saturated spacers. This description is based on the characterization of the evolution of the wire electronic structure as a function of a static electric field applied along the molecular axis, which simulates the driving voltage between the two electrodes in the RTD devices. We illustrate that the main parameters controlling the NDR behavior can be modulated through molecular engineering of the wires.

## 1. Introduction

Soon, the semiconductor industry will start facing difficulties in maintaining the exponential growth with time, experienced over the last thirty years, of the density of transistors packed on a silicon chip.<sup>1–3</sup> This expected deviation from Moore's law is inherent to technological limitations in reducing the size of conventional MOS (Metal/Oxide/Semiconductor) transistors<sup>2</sup> and to the substantial increase in the costs required for manufacturing very large scale integration (VLSI) circuits.<sup>3</sup> The search for alternate routes toward increased miniaturization of electronic circuits has opened the way to the emerging field of molecular electronics. The main challenge here is to establish that single molecules or a finite ensemble of self-assembled molecules can perform all the basic functions of conventional electronic components (i.e., wires, diodes, and transistors).<sup>4</sup> Down the road, this approach can trigger innovative operating schemes, such as in Quantum Cellular Automata (QCA) where the on/off states correspond to different charge configurations of a single molecular unit (rather than to changes in the intensity of a current flowing through a device).<sup>5</sup>

Aviram and Ratner first proposed in 1974 the idea of a molecular rectifier based on organic compounds made of  $\pi$ -donor and  $\pi$ -acceptor moieties linked by a saturated spacer and sandwiched between two metallic electrodes.<sup>6</sup> This concept has recently been verified experimentally.<sup>7,8</sup> Measurements have

also demonstrated that small conjugated molecules, typically phenylene-based derivatives, can behave as a conducting wire when inserted into a metallic break junction<sup>9</sup> or when anchored on a metallic surface and contacted by an STM (Scanning Tunneling Microscopy) tip;<sup>10,11</sup> molecules with asymmetric chemical structures are often observed to display a rectifying behavior.<sup>12–14</sup> Moreover, it has been shown that a current can flow along quantum wires made of carbon nanotubes<sup>15</sup> or DNA molecules<sup>16</sup> positioned between two metallic electrodes.

In parallel, many theoretical efforts have been devoted to the understanding of conduction mechanisms through molecular wires and the simulation of *I/V* characteristics of molecular junctions.<sup>17–22</sup> These studies have addressed the way molecular conductance is affected by (i) the electronic structure of the

(9) Reed, M. A.; Zhou, C.; Muller, C. J.; Burgin, T. P.; Tour, J. M. *Science* **1997**, *278*, 252.

(10) Bumm, L. A.; Arnold, J. J.; Cygan, M. T.; Dunbar, T. D.; Burgin, T. P.; Jones, L., II; Allara, D. L.; Tour, J. M.; Weiss, P. S. *Science* **1996**, *271*, 1705.

(11) Andres, R. P.; Bein, T.; Dorogi, M.; Feng, S.; Henderson, J. I.; Kubiak, C. P.; Mahoney, W.; Osifchin, R. G.; Reifenberger, R. *Science* **1996**, *272*, 1323.

(12) Zhou, C.; Deshpande, M. R.; Reed, M. A.; Tour, J. M. *Appl. Phys. Lett.* **1997**, *71*, 611.

(13) Dhirani, A.; Zehner, R.; Lin, P. H.; Sita, L. R.; Guyot-Sionnest, P. *J. Chem. Phys.* **1997**, *106*, 5249.

(14) Seminario, J. M.; Zacarias, A. G.; Tour, J. M. *J. Am. Chem. Soc.* **2000**, *122*, 3015.

(15) Trans, S. J.; Devoret, M. H.; Dai, H.; Thess, A.; Smalley, R. E.; Geerligs, L. J.; Dekker, C. *Nature* **1997**, *386*, 474.

(16) Porath, D.; Bezryadin, A.; de Vries, S.; C. Dekker, C. *Nature* **2000**, *403*, 635.

(17) Yaliraki, S. N.; Kemp, M.; Ratner, M. A. *J. Am. Chem. Soc.* **1999**, *121*, 3428.

(18) Mujica, V.; Kemp, M.; Ratner, M. A. *J. Chem. Phys.* **1994**, *101*, 6849.

(19) Samanta, M. P.; Tian, W.; Datta, S.; Henderson, J. I.; Kubiak, C. P. *Phys. Rev. B* **1996**, *53*, 7626.

(20) Datta, S.; Tian, W.; Hong, S.; Reifenberger, R.; Henderson, J. I.; Kubiak, C. P. *Phys. Rev. Lett.* **1997**, *79*, 2530.

(21) Magoga, M.; Joachim, C. *Phys. Rev. B* **1996**, *56*, 4722.

(22) Emberly, E. G.; Kirczenow, G. *Phys. Rev. B* **1998**, *58*, 10911.

<sup>†</sup> University of Mons-Hainaut.

<sup>‡</sup> The University of Arizona.

(1) Dagani, R. *Chem. Eng. News* **2000**, January 3, 22.

(2) Packan, P. A. *Science* **2000**, *288*, 319.

(3) Birnbaum, J.; Williams, S. *Phys. Today* **2000**, January, 38.

(4) Reed, M. *Sci. Am.* **2000**, June, 69.

(5) Lent, C. S. *Science* **2000**, *288*, 1597.

(6) Aviram, A.; Ratner, M. A. *Chem. Phys. Lett.* **1974**, *29*, 277.

(7) Metzger, R. M. *Acc. Chem. Res.* **1999**, *32*, 950.

(8) Metzger, R. M.; Chen, B.; Höpfner, U.; Lakshminantham, M. V.; Vuillaume, D.; Kawai, T.; Wu, X.; Tachinaba, H.; Hughes, T. V.; Sakurai, H.; Baldwin, J. W.; Hosch, C.; Cava, M. P.; Brehmer, L.; Ashwell, G. J. *J. Am. Chem. Soc.* **1997**, *119*, 10455.

molecule, (ii) the geometry of the metal/molecule interface and the nature of the chemical interactions, and (iii) the profile of the electrostatic potential across the junction (which can drop abruptly at the interfaces<sup>20</sup>).

Molecules sandwiched between metallic contacts can also be used for the fabrication of molecular resonant tunneling diodes (RTDs).<sup>23,24</sup> The *I/V* characteristics of such devices display at low voltage an NDR (Negative Differential Resistance) behavior (i.e., an initial rise in current followed by a sharp decrease when the voltage is progressively augmented), instead of the linear increase expected from Ohm's law or the staircase behavior reported for molecular junctions.<sup>11</sup> The typical architecture of the RTD devices, originally made of III–V semiconductors, consists of a central quantum well (characterized by discrete and highly spaced electronic levels) separated from two metallic leads by tunnel barriers. The current peak is promoted under the application of a driving voltage by matching the Fermi energy of one electrode to the energy of a discrete electronic level of the quantum well, thus by inducing resonant tunneling processes across the barriers;<sup>25</sup> note that the obtention of sharp peak profiles requires a narrow density of states around the Fermi edge of the electrodes, as is typically found in highly doped inorganic materials or in STM tips. Interestingly, such peak behavior opens the way to the fabrication of novel two-terminal (i.e., NDR diodes) and three-terminal (i.e., NDR transistors) switching devices, which can be further combined with standard electronic components for the design of complex memory or logic circuits, as recently demonstrated with inorganic semiconductors.<sup>26,27</sup>

An NDR behavior is often observed for molecules adsorbed on a gold surface when contacted by a STM tip, as a result of the narrow density of states in the tip electrode.<sup>20</sup> An NDR signature has also been clearly established for two kinds of molecular structures sandwiched in nanopores between two gold surfaces; the mechanisms of electronic switching appear to be different in that case and are not fully understood yet. On one hand, a very sharp NDR behavior with a peak-to-valley ratio of 1030:1 for the current density has been measured at 60 K for a short phenylene–ethynylene oligomer (substituted asymmetrically by  $\pi$ -active groups, see Figure 1a) sandwiched between two gold contacts; interestingly, an NDR behavior with a much lower peak-to-valley ratio was also demonstrated at room temperature for the same conjugated backbone substituted only with the nitro group.<sup>28</sup> The only mechanism proposed to date to explain the NDR behavior for molecules incorporated into nanopores is based on Density Functional Theory (DFT) calculations that have been used to analyze the electronic structure of such molecules in the neutral, singly, and doubly reduced states.<sup>14</sup> The results have been interpreted to suggest that the high current peak is associated to full electronic delocalization of the lowest unoccupied molecular orbital (LUMO) in the singly reduced state; according to this interpretation, the peak profile (i.e., the NDR behavior) results from the absence of delocalization in the neutral and doubly reduced states, such delocalization being required to ensure conductance

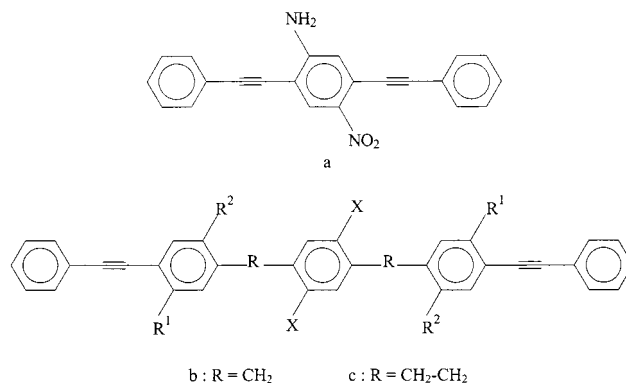


**Figure 1.** Chemical structure of molecular wires for which NDR behavior has been observed experimentally (a and b) and of those under study in the present work (b and c). The substitution pattern considered in the study of derivatives of molecule 1c are also illustrated (the choices of the X, R<sup>1</sup>, and R<sup>2</sup> substituents are described in Table 1).

across the molecular junctions.<sup>14</sup> On the other hand, an NDR behavior has also been observed for compounds where the tunnel barriers leading to resonant tunneling processes are included within the molecular structure.<sup>29</sup> This was evidenced by contacting with two gold electrodes a self-assembled layer of molecular wires made of a benzene, acting as a quantum well, separated from two phenylene–ethynylene segments by tunnel barriers built with methylene spacers, see Figure 1b<sup>4,23</sup> (note that this molecule is also substituted by thioacetyl groups on the para carbon atoms of the external phenylene rings to promote chemisorption on the gold surfaces<sup>23</sup>).

There are two different contributions determining the amplitude of the current across a molecular junction that must be taken into account to simulate *I/V* characteristics.<sup>17,18</sup> The first one is related to the nature of the interaction between the molecule and the metallic surface that governs the mechanisms of charge injection into the wire (ohmic contact versus tunneling); these interfacial reactions are often associated to a contact resistance at the macroscopic level. This interaction also sets the relative position of the Fermi energy of the metal electrodes with respect to the frontier electronic levels of the molecule. The second contribution is related to the extent of delocalization of the electronic levels into which the charges are injected.

The state of the art in the field has not yet reached the stage where *I/V* curves of long molecular wires can be predicted on a quantitative basis. The most sophisticated approaches (typically based on DFT calculations) have been applied so far to small molecules such as benzenedithiol sandwiched between two gold contacts;<sup>30</sup> the large size of the wires under consideration here prevents the use of a similar theoretical approach. Recent DFT calculations have also shown that the addition of sulfur and gold atoms on the terminal carbon atoms of molecule **1a** does not modify the main characteristics of the isolated molecule, thus demonstrating that the interactions between the molecule and the metallic surface are local.<sup>31</sup> In our view, this justifies that there is still a fundamental interest from a theoretical standpoint to address separately, at least in the case of long molecular wires, the charge injection mechanism (i.e., the interfacial interactions between molecules and metallic surfaces<sup>32,33</sup>) and the charge

(23) Reed, M. A. *IEEE Proc.* **1999**, *87*, 652.

(24) Chen, J.; Reed, M. A.; Rawlett, A. M.; Tour, J. M. *Science* **1999**, *286*, 1550.

(25) Abe, M.; Yokoyama, N. *Semiconductor Heterostructure Devices*; Gordon and Breach: New York, 1989.

(26) Mazumder, P.; Kulkarni, S.; Bhattacharya, B.; Sun, J. P.; Haddad, G. I. *IEEE Proc.* **1998**, *86*, 644.

(27) *Technology Roadmap for Nanoelectronics 1999*; edited by Compano, R.; Molenkamp, L.; and Paul, D. J. (European Commission, IST Programme, Future and Emerging Technologies).

(28) Chen, J.; Wang, W.; Reed, M. A.; Rawlett, A. M.; Price, D. W.; Tour, J. M. *Appl. Phys. Lett.* **2000**, *77*, 1224.

(29) Tour, J. M.; Kozaki, M.; Seminario, J. M. *J. Am. Chem. Soc.* **1998**, *120*, 8486.

(30) Derosa, P. A.; Seminario, J. M. *J. Phys. Chem. B* **2001**, *105*, 471.

(31) Seminario, J. M.; Zacarias, A. G.; Derosa, P. A. *J. Phys. Chem. A* **2001**, *105*, 792.

(32) Vondrak, T.; Wang, H.; Winget, P.; Cramer, C. J.; Zhu, X. Y. *J. Am. Chem. Soc.* **2000**, *122*, 4700.

(33) Johanson, A.; Stafström, S. *Chem. Phys. Lett.* **2000**, *322*, 301.

migration process along a conjugated backbone (intimately related to the delocalized versus localized character of the frontier one-electron levels).

In this context, the primary goal of our calculations is to focus on the one-electron structure of the wires and to illustrate on a qualitative basis the way barriers incorporated along the conjugated backbone can lead to an NDR signal (by “qualitative”, we mean that our model will be able to rationalize the peak profile observed in  $I/V$  curves of NDR devices but not to provide absolute numbers for the turn-on voltage and the current, due to the neglect of the metallic contacts). Our results indicate that the origin of the NDR behavior appears to be different here from that reported for the substituted phenylene ethynylene oligomers.<sup>14</sup> We have performed calculations on molecule **1b** for which an NDR behavior has been observed experimentally as well as on molecule **1c** where the methylene spacers are replaced by dimethylene units (the chemical structures are shown in Figure 1). Our calculations further demonstrate that the main parameters controlling the NDR behavior can be fine-tuned through molecular engineering of the wires, in particular upon attachment of electroactive substituents along the conjugated backbone.

## 2. Theoretical Methodology

The geometric structures of molecules **1b** and **1c** have been optimized with the semiempirical Hartree–Fock Austin Model 1 (AM1) method,<sup>34</sup> which has been parametrized to provide accurate geometries for organic molecules in their ground state. In isolated phenylene–ethynylene oligomers, the phenylene rings can easily rotate due to the presence of triple bonds; we have thus assumed that the external segments are planar in molecules **1c** and **1b** as a result of solid-state packing in the self-assembled monolayers. Since we focus on the one-electron properties of the wires, it is seen that the attachment of thiol or thioacetyl groups on the terminal carbon atoms of the external segments hardly affects the results; this issue is therefore not discussed here.

The electronic structures of the molecules have been evaluated with the spectroscopic version of the Hartree–Fock semiempirical Intermediate Neglect of Differential Overlap (INDO/S) Hamiltonian developed by Zerner and co-workers.<sup>35,36</sup> The reliability of the INDO approach to describe the relative positions and characteristics of the occupied and unoccupied levels of organic conjugated materials has been assessed, among others, in a number of our previous theoretical studies;<sup>37–42</sup> remarkable agreement has, for instance, been found between the experimental Ultraviolet Photoelectron Spectroscopy (UPS) and Inverse Photoemission Spectroscopy (IPES) data and the INDO-simulated spectra for several organic conjugated molecules.<sup>43,44</sup> This

(34) Dewar, M. J. S.; Zoebisch, E. G.; Healy, E. F.; Stewart, J. J. P. *J. Am. Chem. Soc.* **1995**, *107*, 3702.

(35) Ridley, J.; Zerner, M. C. *Theor. Chim. Acta* **1973**, *32*, 111.

(36) Zerner, M. C.; Loew, G. H.; Kichner, R.; Mueller-Westerhoff, U. T. *J. Am. Chem. Soc.* **1980**, *102*, 589.

(37) Brédas, J. L.; Cornil, J.; Meyers, F.; Beljonne D. In *Handbook of Conducting Polymers*, 2nd ed.; Skotheim, T. A., Reynolds, J. R., Elsenbaumer, R. L., Eds; Marcel Dekker: New York, 1997; p 1.

(38) Marder, S. R.; Gorman, C. B.; Meyers, F.; Perry, J. W.; Bourhill, G.; Brédas, J. L.; Pierce, B. M. *Science* **1994**, *265*, 632.

(39) Meyers, F.; Marder, S. R.; Pierce, B. M.; Brédas, J. L. *J. Am. Chem. Soc.* **1994**, *116*, 10703.

(40) Marder, S. R.; Torruellas, W. E.; Blanchard-Desce, M.; Ricci, V.; Stegeman, G. I.; Gilmour, S.; Brédas, J. L.; Li, J.; Bublitz, G. U.; Boxer, S. G. *Science* **1997**, *276*, 1233.

(41) Maertens, C.; Detrembleur, C.; Dubois, P.; Jérôme, R.; Boutton, C.; Persoons, A.; Kogej, T.; Brédas, J. L. *Chem. Eur. J.* **1999**, *5*, 369.

(42) Beljonne D.; Shuai, Z.; Cornil, J.; dos Santos, D. A.; Brédas, J. L. *J. Chem. Phys.* **1999**, *111*, 2829.

(43) Cornil, J.; Vanderdonck, S.; Lazzaroni, R.; dos Santos, D. A.; Thys, G.; Geise, H. J.; Yu, L. M.; Szablewski, M.; Bloor, D.; Lögdlund, M.; Salaneck, W. R.; Gruhn, N. E.; Lichtenberger, D.; Lee, P. A.; Armstrong, N. R.; Brédas, J. L. *Chem. Mater.* **1999**, *11*, 2436.

(44) Hill, I. G.; Kahn, A.; Cornil, J.; dos Santos, D. A.; Brédas, J. L. *Chem. Phys. Lett.* **2000**, *317*, 444.

gives confidence that the INDO Hamiltonian can provide a reliable description of the one-electron structure of organic conjugated materials, which is a key ingredient of our model. We note that the energy separation between the occupied and unoccupied levels, and thus the HOMO to LUMO gap, is overestimated in any Hartree–Fock-based calculations; however, it is important to stress that this drawback does not impact the model proposed in this work to rationalize the NDR behavior since this model depends on the nature of the highest occupied or lowest unoccupied levels and not on the separation in HOMO to LUMO gap.

Resonant tunneling processes across the barriers formed by the saturated spacers are identified by examining the evolution of the one-electron structure of the wires under the application of a static electric field aligned along the main molecular axis. This field is used to simulate the voltage across the electrodes in the RTD devices and to induce a linear evolution of the electrostatic potential along the wire; this, in turn, modulates the relative energies of the electronic levels originating in the three conjugated moieties, as exemplified below. In our calculations, the gradient of potential energy is created around the origin of the Cartesian axes chosen to be at the center of the middle benzene ring; with this choice, the energies of the electronic levels located on the quantum well are slightly affected by the electric field, as is also expected in RTD devices built with molecules connected to two symmetric contacts. The negative pole of the driving voltage is positioned on the left side of the molecule so that the field induces a destabilization [stabilization] of the electronic levels localized on the left [right] part of the wire with respect to the situation in the absence of external perturbation. The amplitudes of the applied electric field used in the calculations cannot be directly compared to the experimental voltages, partly because we do not consider the chemical interactions and possible voltage drops at the metal/organic interfaces.<sup>20</sup>

Our approach is triggered by previous theoretical studies showing that the main characteristics of the evolution in the electronic and optical properties of conjugated chromophores under the influence of an external polarization (created for instance by a solvent or adjacent molecules in a condensed medium) can be well described by the simple application of a static electric field.<sup>38–42</sup>

## 3. Results and Discussion

Since the evolution of the electronic structure of the molecular wires under the influence of a static electric field plays a major role in the understanding of the resonant tunneling processes, we first depict the nature of the highest occupied and lowest unoccupied levels in molecule **1c** in the absence of field; the levels, which are the most relevant to the NDR behavior, are illustrated in Figure 2 together with the corresponding one-electron levels calculated in the isolated segments. Analysis of Figure 2 reveals that the lowest two unoccupied levels of the wire (LUMO and LUMO+1) are mostly localized on the external conjugated segments and originate from the bonding and antibonding interaction of the lowest  $\pi$ -unoccupied level of the external units. These two levels are almost degenerate due to the large separation between the two moieties following the incorporation of the central quantum well surrounded by two tunnel barriers; as a consequence, any slight external perturbation is expected to localize the electronic wave function on a single conjugated segment of the wire. The same description prevails for the LUMO+2 and LUMO+3 as well as for the LUMO+4 and LUMO+5 levels described by the linear combination of higher lying unoccupied levels localized on the external units. Similarly, examination of the occupied levels shows that the highest two molecular orbitals (HOMO and HOMO-1) are localized on the external segments.

In addition to these molecular levels localized on the external conjugated units, we find two occupied (HOMO-2 and HOMO-3)  $\pi$ -levels and two unoccupied  $\pi^*$ -levels (LUMO+6 and LUMO+7) mostly centered on the benzene quantum well.



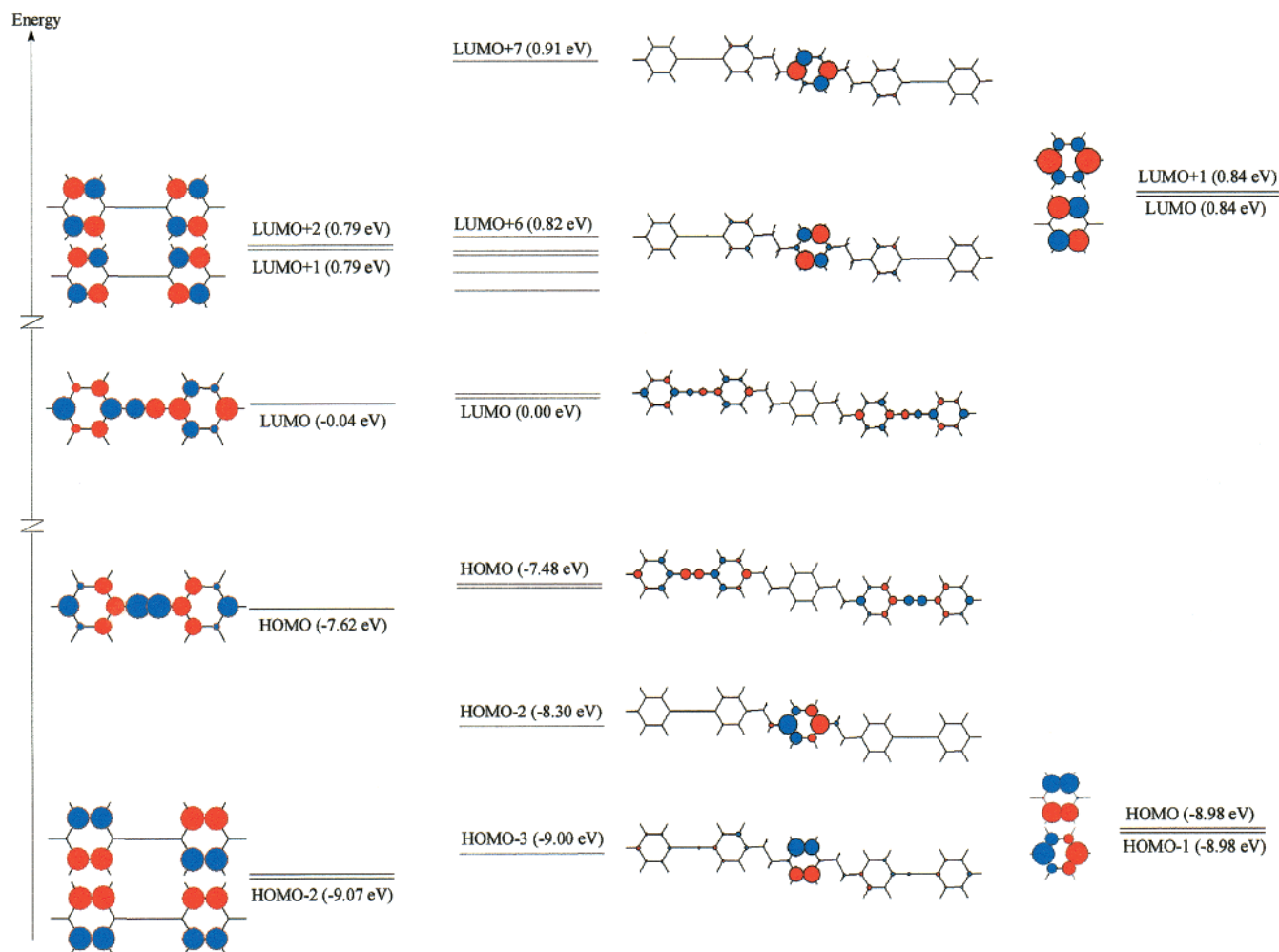


**Figure 2.** Description at the INDO level of the nature of the highest occupied and lowest unoccupied  $\pi$ -molecular levels in molecule **1c** as well as in the isolated individual segments in the absence of external electric field. The size and color of the circles correspond to the amplitude and sign, respectively, of the LCAO (Linear Combination of Atomic Orbitals) coefficients associated with the  $\pi$ -atomic orbitals of the carbon atoms in the conjugated backbone.

Among these, the levels characterized by a vanishingly small electronic density on the para carbon atoms of the benzene ring (HOMO-3 and LUMO+6) have energies very similar to those calculated in the isolated molecule, since they are only weakly affected by para substitutions. In contrast, the LUMO+7 level has significant LCAO coefficients on the para carbon atoms of the central ring and is slightly destabilized with respect to the corresponding orbital in the isolated molecule, due to inductive effects from the dimethylene spacers within the  $\sigma$ -skeleton. Thus, the para substitution of the central benzene unit in the wire breaks the level degeneracy present in the isolated molecule and creates a small energy gap on the order of 0.09 eV between the lowest two unoccupied levels lying on the quantum well. Note that the splitting is much more pronounced in the case of the HOMO-2 and HOMO-3 levels, on the order of 0.7 eV. This evolution is consistent with the results of INDO calculations showing the appearance of the same splittings when going from benzene to paraxylene.

Analysis of the one-electron levels thus confirms that molecule **1c** can be regarded as consisting of three weakly interacting conjugated units. In the following, we illustrate the origin of NDR behavior in such a molecule by considering that at low voltage an electron [hole] is initially injected into the lowest unoccupied [highest occupied] level of the left [right] external segment of the wire before any resonant tunneling

process can occur. In such a scenario, the charge has time to geometrically relax under the form of a negative or positive polaron. The explicit consideration of such relaxations is, however, not of fundamental importance here since their only impact is to induce a stabilization [destabilization] by a few tenths of an electronvolt of the lowest unoccupied [highest occupied] level of the external segment upon electron [hole] injection;<sup>45</sup> this would thus lead to a slight variation in the voltages required to activate the various resonant channels. Moreover, since the size of the phenylene-ethynylene segment is equivalent to that of a positive or negative polaron,<sup>45</sup> the formation of such species does not lead to marked changes in the shapes of the orbitals (such as, for instance, appearance of localization of the electronic wave function, as could be observed in longer chains), which otherwise might have played a significant role in the interpretation of the NDR signature.

When electrons [holes] are initially injected into the lowest unoccupied [highest occupied] level of the left [right] external segment of the wire, the current across the junction is expected to be vanishingly small. The reason for this is 2-fold: (i) efficient charge transfer toward a level on the opposite external segment through a superexchange (i.e., through-space) mechanism can hardly take place due to the significant separation between the

(45) Brédas, J. L.; Street, G. B. *Acc. Chem. Res.* **1985**, *18*, 309.

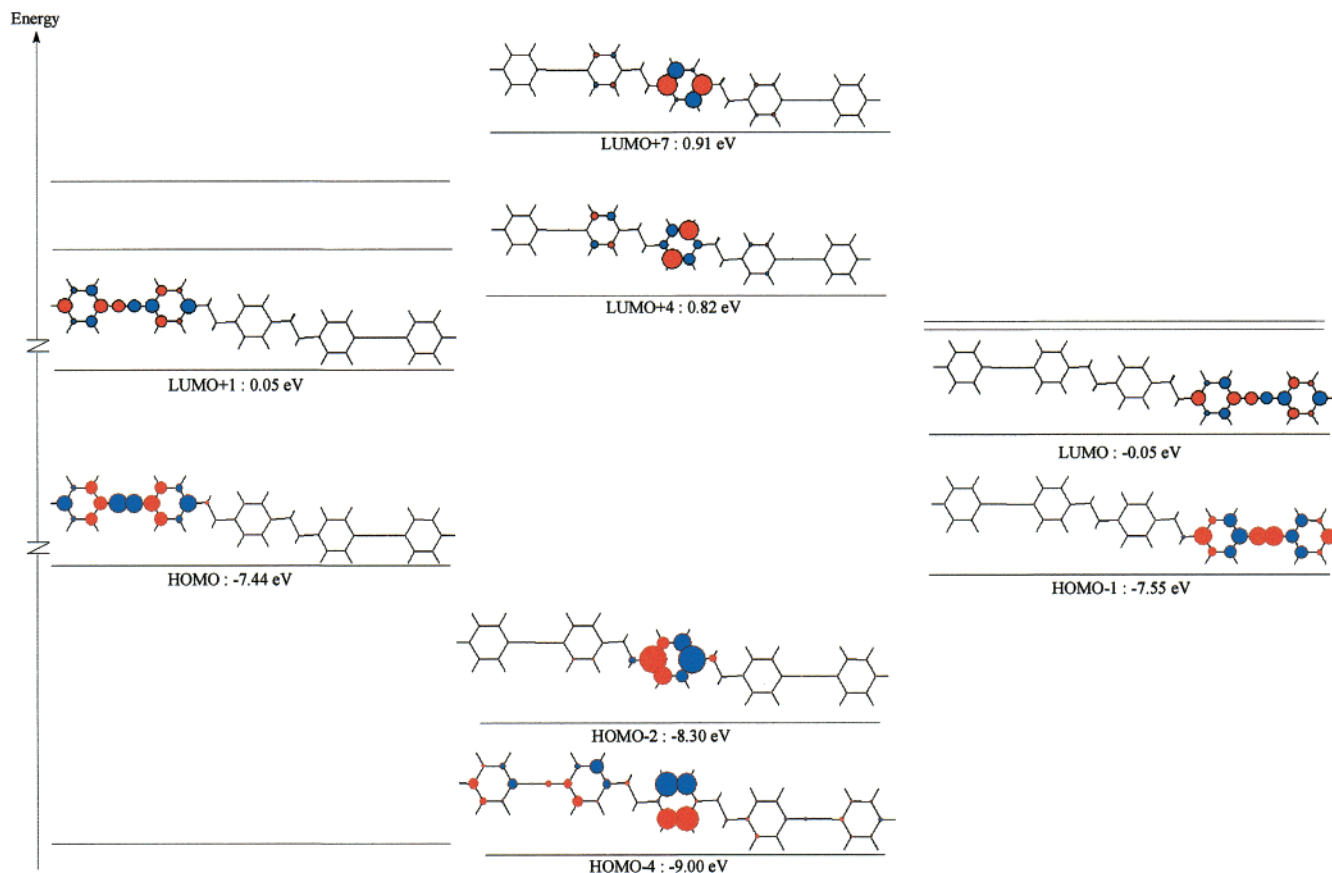


**Figure 3.** INDO-calculated one-electron structure of molecule **1c** under the application of a static electric field of  $5 \times 10^5$  V/cm. The wave functions are illustrated for the levels most relevant to NDR behavior; the levels are classified in three columns depending on their localization on the wire.

two units (on the order of  $10 \text{ \AA}$ ) and the decreasing exponential dependence of the electron-transfer rate as a function of distance,<sup>46</sup> and (ii) a through-bond mechanism involving a level of the quantum well much higher [lower] in energy implies a very large energy barrier to overcome. The easiest way to promote a current across the wire is thus to modulate the relative energies of electronic levels belonging to the different conjugated segments upon application of a voltage, to generate a resonant tunneling process across the tunnel barriers created by the saturated spacers. This points to the fundamental interest in characterizing the evolution of the electronic structure of the wire as a function of a static electric field, as discussed below.

The evolution of the one-electron structure of molecule **1c** under the application of a static electric field of  $5 \times 10^5$  V/cm is depicted in Figure 3, where the levels are displayed in three columns according to their localization on the molecule; note that the amplitude of the electric field is much lower than that required to reach the first resonance. The linear evolution of the electrostatic potential along the whole molecule leads to removal of the degeneracy of the electronic levels localized on the two external segments in the absence of the field. As expected, the results show that the energy separation between the lowest unoccupied [highest occupied] level on the left [right] conjugated segment and the lowest unoccupied [highest occupied] level of the central well is reduced upon application of a static electric field along the molecule. Figure 4 further illustrates that the destabilization [stabilization] of the lowest unoccupied [highest occupied] level of the left [right] segment

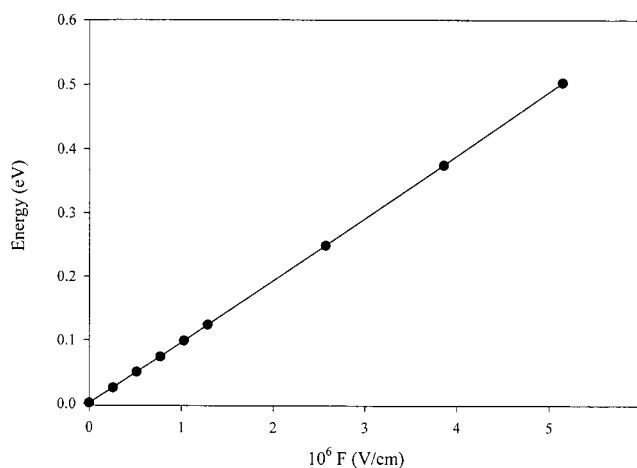


**Figure 4.** Evolution of the INDO energy of the lowest unoccupied level on the left external segment of the wire as a function of the amplitude of the static electric field aligned along the long molecular axis.

evolves linearly with the electric field; this allows us to establish that an increase by  $\sim 5 \times 10^5$  V/cm in the amplitude of the field leads in our calculations to a corresponding shift of the frontier levels by 0.05 eV.

When a critical field of  $9 \times 10^6$  V/cm is applied, we observe a first resonant tunneling process, which takes place between the lowest unoccupied level on the left conjugated segment and that of the quantum well. This resonance generates two electronic levels (LUMO+4 and LUMO+5) characterized by a bonding and antibonding combination, with equal weight, of

(46) Barbara, P. F.; Meyer, T. J.; Ratner, M. A. *J. Phys. Chem.* **1996**, *100*, 13148.

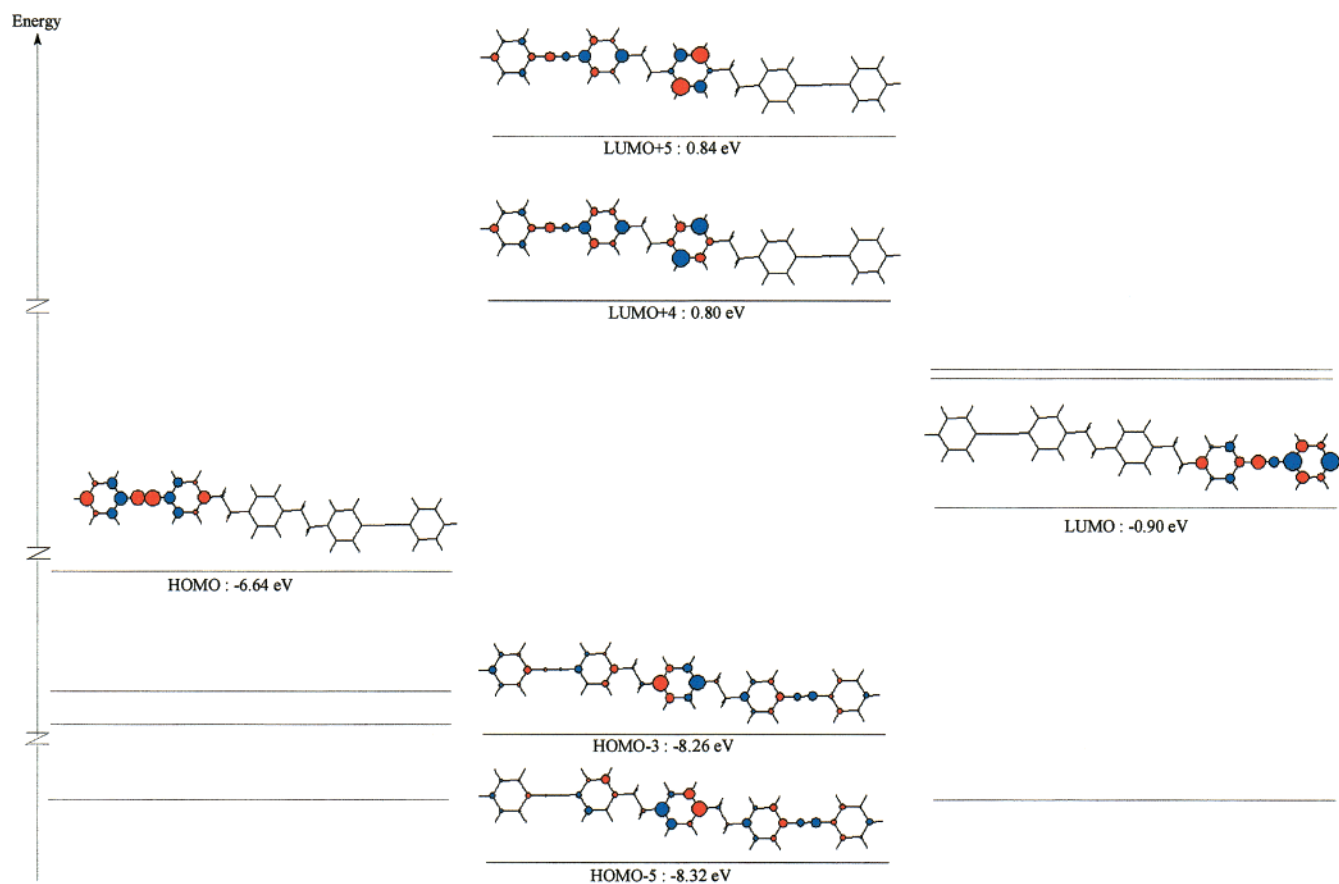


**Figure 5.** INDO-calculated one-electron structure of molecule **1c** under the application of a critical field inducing resonances between the lowest unoccupied [highest occupied] level of the left [right] external segment and the lowest unoccupied [highest occupied] level of the central benzene unit. The levels are classified in three columns depending on their localization on the wire; note that the HOMO-4 level has a significant electronic density on the two external segments.

the levels characteristic of the individual units (see Figure 5). The rate of electron transfer (and hence the current) between the left conjugated segment and the central quantum well is expected to be by far the highest at the resonance; this allows us to rationalize in a qualitative way the peak profile observed in the experimental  $I/V$  curves.<sup>23</sup> Indeed, prior to or after the resonance there is an offset between the two electronic levels involved in the charge transfer; the electron transfer process is then considerably slowed by the fact that vibrations must come into play to reach a transition state where the two levels acquire the same energy; in this situation, the rate of charge transfer can be estimated in the framework of Marcus theory, with an explicit account of vibrational contributions.<sup>46</sup> In contrast, at the resonance, the transfer is not assisted by vibrations since the two levels have the same energy; the strength of the electronic coupling between the two segments is the main parameter governing the charge-transfer rate, as is the case in models describing transport properties in a band regime (where current flows under the form of unrelaxed charge carriers).<sup>47,48</sup> This coupling is quantified by the transfer integral between the two segments (the larger the transfer integral, the higher the transfer rate), which can be estimated in first approximation as half the energy splitting between the two resonant orbitals;<sup>49</sup> we calculate a transfer integral on the order of 20 meV for the

resonance occurring between the lowest unoccupied level of the left conjugated segment and that of the central quantum well. We note, by analogy, that the same considerations apply to the charge mobility in molecular crystals: the mobility is much higher at low temperature (where a band-like motion prevails) than at high temperature (where transport is described in terms of phonon-assisted hopping processes of relaxed charges between adjacent molecules); in ultrapure single crystals of pentacene, there occurs an increase in charge mobility by up to 5 orders of magnitude when going from the high- to the low-temperature regime.<sup>50,51</sup>

Of course, the resonance between the lowest unoccupied level of the left segment and that of the central benzene ring does not ensure alone the switching on of a high current across the whole junction; high current additionally requires a significant electronic coupling (i.e., a small energy separation) between the lowest resonant level and an unoccupied level located at lower energy on the right segment of the wire; this condition is not met here since the smallest separation is on the order of 0.6 eV. However, Figure 5 also shows that the first resonance in the manifold of the unoccupied levels coincides with another resonance taking place between the highest occupied level on the quantum well and that of the right conjugated segment; this is consistent with the fact that the energy separations between the corresponding frontier levels (LUMO vs LUMO+6 and HOMO vs HOMO-2) are very similar (0.82 eV) in the one-

(47) Haddon, R. C.; Siegrist, T.; Fleming, R. M.; Bridenbaugh, P. M.; Laudise, R. A. *J. Mater. Chem.* **1995**, *5*, 1719.

(48) Pope, M.; Swenberg, C. E. *Electronic Processes in Organic Crystals and Polymers*; Oxford University Press: New York, 1999.

(49) Li, X. Y.; Tang, X. S.; He, F. C. *Chem. Phys.* **1999**, *248*, 137.

(50) Schön, J. H.; Kloc, C.; Batlogg, B. *Science* **2000**, *288*, 2388.

(51) Schön, J. H.; Berg, S.; Kloc, C.; Batlogg, B. *Science* **2000**, *287*, 1022.

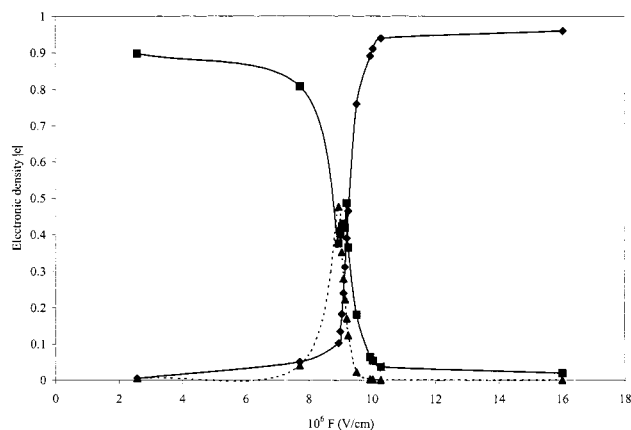


**Figure 6.** INDO-calculated evolution of the distribution of the electronic density over the three conjugated segments of molecule **1c** (filled squares, central well; filled diamonds, right segment; filled triangles, left segment) in the HOMO-3 level as a function of the amplitude of the static electric field around the critical value activating the efficient hole transport channel (the values reported in the plot do not include the weak contribution arising from the saturated spacers).

electron structure of the molecule in the absence of electric field, see Figure 2. The transfer integral associated to this resonance is on the order of 30 meV.

Most importantly, the two resonant levels are found to interact here also with an electronic level on the left side of the wire; this is reflected in Figure 5 by the appearance in the resonant orbitals of a significant electronic density over the *three* segments of the molecular wire. The activation of this hole resonant channel is further illustrated in Figure 6 where we have reported the distribution of the electronic density among the three conjugated segments in the HOMO-3 level as a function of the electric field around the critical value. The evolution shows that the electronic level is localized on the quantum well prior to the resonance, gets delocalized over the three moieties around the critical field, and finally becomes localized on the right external segment beyond the resonance. On the basis of these results, we can thus conclude that the resonances occurring at the lowest critical field give rise to a much more efficient transport channel across the molecular junction for holes than for electrons; note that the actual current observed in the *I/V* curves upon activation of the hole channel will actually depend on the efficiency of the charge injection process into the highest occupied level of the right segment.

A slightly larger electric field (or voltage) has to be applied to promote the resonance between the lowest unoccupied level of the left segment and the second unoccupied level of the benzene ring (at 0.09 eV above its lowest unoccupied level); a further increase in the amplitude of the electric field ( $18 \times 10^6$  V/cm) is required to achieve a hole resonant tunneling process between the highest occupied level of the right conjugated segment and the second occupied level of the quantum well (at 0.7 eV below its highest occupied level). These two channels appear to be rather inefficient for electron [hole] transfer across the molecular junction due to the large energy separation of 0.7 eV [1.0 eV] between the lowest [highest] resonant level and the closest electronic level on the right [left] external segment at lower [higher] energy; this is also reflected by the absence of electronic delocalization over the whole  $\pi$ -backbone at the resonance.

Our results thus lead to the conclusion that among the four accessible resonant channels in molecule **1c** (two for electrons and two for holes), only the one involving the highest occupied

level of the benzene ring contributes to a high current (with holes as the charge carriers) across the junction and the observation of an intense current peak in the *I/V* curve. The resonances occurring at different voltages would be individually identified in the experimental *I/V* characteristics if they were all to promote a similar amount of current across the junction. The activation of several channels might induce a broadening of the NDR peak if the resonances take place in a limited voltage range; this would, however, prevent a fine control of the switching process. Other possible sources of broadening of the NDR peak neglected in the present calculations are related to (i) the dispersion of the electronic levels due to intermolecular interactions<sup>52</sup> between the conjugated segments within the self-assembled monolayers (SAMs) and (ii) a distribution in the energy of the frontier molecular levels of the external segments due to various kinds of interaction between the molecules and the gold surface.

Much higher electric fields help in reaching the highest unoccupied level of the benzene ring (2.3 eV above its lowest unoccupied level) or the lowest occupied level (4.0 eV below its highest occupied level). However, these levels are not expected to induce an NDR behavior due to the fact that they are surrounded by  $\sigma$ -levels delocalized over the whole backbone. The manifold of these delocalized  $\sigma$ -levels (whose energies are only slightly affected by the field due to their delocalization over the molecular backbone) contributes to the transport of electrons and holes through the  $\sigma$ -skeleton without the need for resonant tunneling processes across the dimethylene barriers; in this regime, we thus expect a continuous increase in the conductance through the wire when the voltage is amplified.

We now turn to the analysis of the one-electron structure and characterization of the NDR behavior in the molecular wire incorporating methylene units as conjugation breakers (Figure 1b). To do so, we describe in Figure 7 the nature of the most relevant electronic levels of the molecule in the absence of electric field. The one-electron structure differs from that of molecule **1c** since (i) we calculate a finite electronic density on the quantum well in both the HOMO and LUMO levels of the molecule (this should contribute to a leakage current across the junction prior to any resonant tunneling process) and (ii) we find several occupied and unoccupied levels resulting from coincidental resonances between electronic levels belonging to the central well and the external units, and hence delocalized over the whole molecule. This seemingly makes the mechanisms leading to the NDR behavior more complex than for molecule **1b**; however, electronic levels mostly localized on the benzene ring can be identified as soon as a static electric field is applied, following the changes in the relative energies of the electronic levels characteristic of the three different conjugated moieties. The mechanism of the NDR behavior in molecule **1b** is thus very similar to that described in the case of molecule **1c**.

In molecule **1b**, the first resonance occurs between the highest occupied level of the right conjugated segment and that of the central benzene ring (having a significant electronic density on the substituted para carbon atoms). Despite the stronger interaction between the conjugated units, a static electric field much larger than the one used in the case of molecule **1c** has to be applied to promote the first resonance. This counter-intuitive effect is primarily related to the reduction in the length of the saturated spacers when going from molecule **1c** to **1b**; as a matter of fact, a shorter spacer requires a larger slope in electrostatic potential (and hence a higher voltage) for similar

(52) Cornil, J.; Calbert, J. P.; Beljonne, D.; Silbey, R.; Brédas, J. L. *Adv. Mater.* **2000**, *12*, 978.



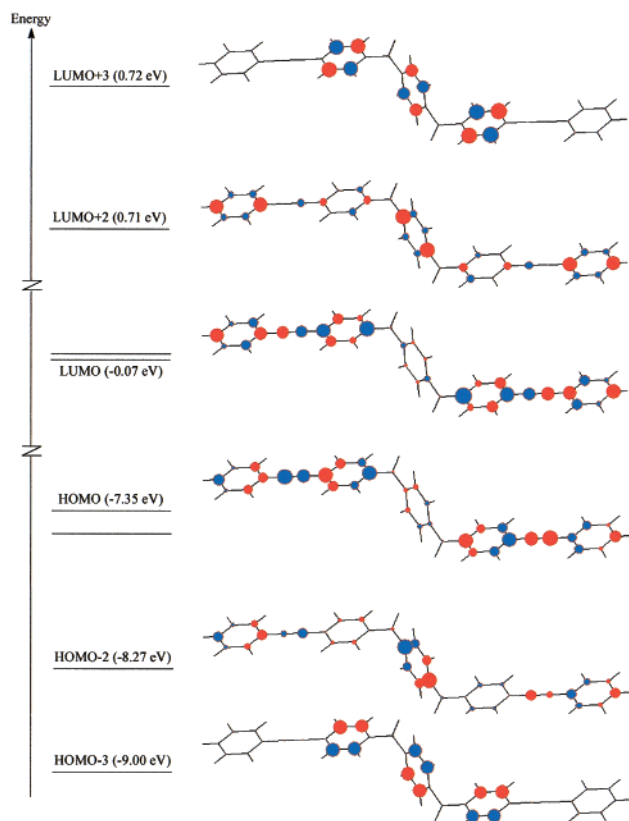


**Figure 7.** Description of the nature of the INDO highest occupied and lowest unoccupied levels of molecule **1b** in the absence of any external electric field. The size of the circles on the quantum well represents the amplitude of the LCAO coefficients associated with the  $p_z$  atomic orbitals of the carbon atoms, with the  $z$  axis being perpendicular to the plane of the external conjugated segments.

energy barriers between frontier levels to be overcome. The smaller spatial separation between the two conjugated segments also leads to much larger transfer integrals with respect to the corresponding values in molecule **1c** (250 meV vs 30 meV).

**Table 1.** INDO-Calculated Energies (in eV) of the Frontier Levels Localized on the External Segments (HS and LS) and the Quantum Well (HB1, HB2, LB1, LB2) of the Molecular Wire Incorporating Dimethylene Spacers and in Various Substituted Derivatives (in the absence of a static electric field)<sup>a</sup>

X	R <sup>1</sup>	R <sup>2</sup>	HS	LS	HB1	HB2	LB1	LB2	Δ1	Δ2	Δ3	Δ4
H	H	H	-7.48	0.00	-8.30	-9.00	0.82	0.91	0.82	0.91	0.82	1.52
H	CH <sub>3</sub>	H	-7.42	0.04	-8.28	-9.00	0.83	0.92	0.79	0.88	0.86	1.58
H	CH <sub>3</sub>	CH <sub>3</sub>	-7.39	0.05	-8.27	-8.99	0.84	0.93	0.79	0.88	0.88	1.60
H	OCH <sub>3</sub>	H	-7.35	0.04	-8.36	-9.07	0.75	0.85	0.71	0.81	1.01	1.72
H	OCH <sub>3</sub>	OCH <sub>3</sub>	-7.29	0.03	-8.23	-8.94	0.88	0.97	0.85	0.94	0.94	1.65
H	CN	H	-7.70	-0.43	-8.46	-9.14	0.67	0.75	1.10	1.18	0.76	1.44
H	CN	CN	-7.92	-0.90	-8.51	-9.18	0.65	0.71	1.55	1.61	0.59	1.26
CH <sub>3</sub>	H	H	-7.48	0.01	-7.99	-8.63	0.90	0.97	0.89	0.96	0.51	1.15
OCH <sub>3</sub>	H	H	-7.46	0.02	-7.81	-8.80	0.80	0.88	0.78	0.86	0.35	1.34
Cl	H	H	-7.53	-0.05	-8.81	-9.46	0.10	0.31	0.15	0.36	1.28	1.93

<sup>a</sup> The positions of the R1, R2, and X substituents are depicted in Figure 1c. We also collected the energy barriers (Δ1→4) calculated between the frontier levels, as illustrated in the sketch on top of the table.

Both the large transfer integral and the overall delocalization of the resonant levels contribute to the creation of a very efficient hole transport channel across molecule **1b**.

In contrast, resonance between the highest occupied level of the right segment and the second occupied level of the benzene ring generates a much less operative channel for holes due to (i) a very small transfer integral ( $\sim 2$  meV), which results both from the absence of electronic density on the para carbon atoms of the central ring and the weak global overlap in the chairlike geometry of the wire between the  $\pi$ -atomic orbitals of the carbon atoms of the two rings connected by the spacer, and (ii) the absence of delocalization of the resonant molecular levels over the whole molecular backbone. When focusing on the unoccupied orbitals of the quantum well, we identify a *single* resonance associated with very large interchain transfer integrals ( $\sim 200$  meV) between the lowest unoccupied level on the left segment and that on the benzene ring characterized by a significant electronic density on the para carbon atoms. This channel operates at a static field slightly larger than that required for tunneling through the highest occupied level of the benzene ring; however, this channel is expected to be much less efficient due to the localized character of the resonant levels. Resonant tunneling across the second unoccupied  $\pi$ -level of the benzene ring (that has a small electronic density on the para carbon atoms and leads to very small interchain transfer integrals) is prevented here by the fact that the energy separation between the lowest two unoccupied levels is much smaller than the transfer integrals associated to the resonance through the delocalized level of the benzene ring; thus, we only observe the interaction with the level of the quantum well possessing a high electronic density on the para carbon atoms in this energy range. All together, we conclude that a single channel is expected to promote a high current (with holes as charge carriers) across molecule **1b**, as is also the case for molecule **1c**.

Finally, we would like to illustrate that the voltages required to promote the individual resonances can be fine-tuned through molecular engineering of the wire. In particular, previous theoretical calculations performed on polyphenylene-based chains have shown that the positions of the frontier levels can



be controlled upon attachment of electroactive substituents on the conjugated backbone.<sup>53,54</sup> We demonstrate below that similar strategy can be applied to molecule **1c** (and by extension to any molecular wire incorporating saturated spacers) to modulate its one-electron structure. Table 1 reports the changes in the energies of the frontier levels localized on the external segments (HS and LS) and those of the highest two occupied (HB1 and HB2) and lowest two unoccupied (LB1 and LB2) levels of the benzene ring under various substitution patterns. The versatility of molecular engineering is illustrated in the following by considering substituents traditionally used by synthetic chemists (methoxy, methyl, and cyano groups as well as chlorine atoms), which are attached either to the central benzene ring or to the inner phenylene ring of the external segments, to avoid steric hindrance at the interface during chemisorption (see Figure 1). Table 1 also collects the four energy barriers ( $\Delta 1 \rightarrow 4$ ) that have to be overcome by the electric field to promote the individual resonances.

The results show that the  $\sigma$ -donor methyl groups attached on the external segments lead to an overall slight destabilization of the levels without affecting the heights of the energy barriers. Similarly, the global influence of the methoxy groups, having  $\pi$ -donor and  $\sigma$ -acceptor characters (the former destabilizes the frontier electronic levels while the latter has a counter-acting effect), is to weakly shift all the frontier levels without significant fluctuations in the energy barriers. The  $\pi$ -acceptor and  $\sigma$ -acceptor characters of the cyano groups both contribute to a significant lowering of the frontier levels; this leads to a significant increase [decrease] in the energy barriers for electron [hole] transfer across the tunnel barrier. These calculated shifts are expected to be amplified when substituting a much smaller conjugated segment; this is confirmed by the results presented in Table 1 showing that the substitution of the central benzene ring yields much larger shifts of the levels with respect to those calculated in the previous cases. Interestingly, the calculations demonstrate that the energy barrier  $\Delta 3$  [ $\Delta 1$ ] associated to the first resonance channel for holes [electrons] can be considerably reduced by the attachment of methoxy groups [attachment of chlorine atoms having  $\pi$ -acceptor and  $\sigma$ -acceptor characters]. Note that the attachment of cyano or aldehyde groups to the central ring leads to a situation where the lowest unoccupied level of the wire is localized on the quantum well.

#### 4. Conclusions

In this work, we have shown that the mechanisms leading to NDR behavior in molecular wires incorporating spacers can be unraveled from the evolution of their one-electron structure upon

application of a static electric field aligned along the long molecular axis. When benzene is used as the central quantum well, resonant tunneling processes through the highest two occupied and lowest two unoccupied levels of the ring are at the origin of the current peaks observed in the  $I/V$  characteristics. The effectiveness of each transport channel is governed by the amplitude of the transfer integral between the levels in interaction at the resonance as well as the degree of delocalization of the resonant levels over the whole molecular backbone. Our calculations indicate that the channel involving the highest occupied level of the benzene ring is the most efficient in the molecular wires under study.

The use of short spacers such as methylene units favors very large interchain transfer integrals at the resonance but prevents a full localization of the frontier levels on the individual segments in the absence of electric field; this should lead to the appearance of a significant valley current in the  $I/V$  characteristics, which is detrimental for the design of memory cells based on molecular RTD devices.<sup>55</sup> In contrast, the incorporation of larger spacers such as dimethylene groups induces a strong confinement of the electronic levels on a given segment of the wires and leads to smaller interchain transfer integrals between resonant levels, and hence to a much lower tunnel current across the molecule. We have also established that the energy barriers to be overcome for the activation of the resonant tunneling channels can be fine-tuned through molecular engineering of the wires, in particular upon attachment of substituents over the conjugated backbone. Our theoretical study is now awaiting experimental  $I/V$  characteristics on a wide range of molecular wires incorporating saturated spacers; this would allow us to critically confront our theoretical results to experimental data and assess the validity of our working hypotheses.

**Acknowledgment.** The authors acknowledge very stimulating discussions with S. Bengtsson, J. Berg, C. Ford, N. C. Greenham, D. J. Paul, M. A. Ratner, P. Sazio, and K. Stokbro. The work in Mons is supported by the Belgian Federal Government "Pôle d'Attraction Interuniversitaire en Chimie Supramoléculaire et Catalyse, PAI 4/11", the Belgian National Fund for Scientific Research (FNRS), and the European Commission project SANEME (under the framework of the 5th IST program, contract number IST-1999-10323). The work at Arizona is partly supported by the National Science Foundation (CHE-0071889) and an IBM Shared University Research grant. J.C. is a Research Associate of the FNRS.

JA010152+

(53) Cornil, J.; dos Santos, D. A.; Beljonne, D.; Brédas, J. L. *J. Phys. Chem.* **1995**, *99*, 5604.

(54) Brédas, J. L.; Heeger, A. J. *Chem. Phys. Lett.* **1994**, *217*, 507.

(55) Berg, J.; Bengtsson, S.; Lundgren, P. *Solid-State Electron.* **2000**, *44*, 2247.